# Observing complex bound states in the spin-1/2 Heisenberg XXZ chain using local quantum quenches

Martin Ganahl,[1] Elias Rabel,[1, 2] Fabian H.L. Essler,[3] and H.G. Evertz[1, *]

[1]*Institut für Theoretische Physik, Technische Universität Graz, Petergasse 16, 8010 Graz, Austria*
[2]*Institut für Festkörperforschung, Forschungszentrum Jülich, 52425 Jülich, Germany*
[3]*The Rudolf Peierls Centre for Theoretical Physics, Oxford University, Oxford OX1 3NP, UK.*

We consider the non-equilibrium evolution in the spin-1/2 XXZ Heisenberg chain for fixed magnetization after a *local quantum quench*. This model is equivalent to interacting spinless fermions. Initially an infinite magnetic field is applied to $n$ consecutive sites and the ground state is calculated. At time $t = 0$ the field is switched off and the time evolution of observables such as the z-component of spin is computed using the Time Evolving Block Decimation (TEBD) algorithm. We find that the observables exhibit strong signatures of linearly propagating spinon and bound state excitations. These persist even when integrability-breaking perturbations are included. Since bound states ("strings") are notoriously difficult to observe using conventional probes such as inelastic neutron scattering, we conclude that local quantum quenches are an ideal setting for studying their properties. We comment on implications of our results for cold atom experiments.

Cold atomic gases provide an ideal testing ground for non-equilibrium many-body quantum physics because the dynamics remains coherent for long times by virtue of the weak coupling to the environment. Recent experiments [1, 2] have opened up the study of an entirely new regime in many particle quantum physics. The "quantum Newton's cradle" experiments of Kinoshita et al drew attention to the importance of dimensionality and conservation laws and prompted a huge number of theoretical analyses on the role played by quantum integrability [3, 4]. A standard protocol for driving a quantum system out of equilibrium is by means of a quantum quench (QQ): a system is prepared in the ground state of a given Hamiltonian $H_0$. At time $t = 0$ an experimentally tuneable parameter that characterizes the Hamiltonian (e.g. a magnetic field) is changed suddenly and one then considers the unitary time evolution of the system by means of the new Hamiltonian $H$. QQs can be either global or local and we focus on the latter case in the following. A particular case of a local QQ is given by the X-ray edge singularity, which is a central paradigm of many-body physics. The types of problems we consider below can be viewed as generalizations of X-ray edge problems, the most crucial difference arising from the initial state and the kind of observable that we consider, which can be measured e.g. in realizations based on cold atomic gases.

We consider the anisotropic spin-1/2 Heisenberg chain on a lattice with $N$ sites with fixed numbers $N_{\uparrow,\downarrow}$ of up and down spins and open boundary conditions [22])

$$H(\Delta, B_0) = J \sum_{i=1}^{N-1} S_i^x S_{i+1}^x + S_i^y S_{i+1}^y + \Delta S_i^z S_{i+1}^z$$
$$- B_0(t) \sum_{i=i_0}^{i_0+m_0-1} S_i^z, \qquad (1)$$

where $J > 0$ and $B_0$ is a local magnetic field acting on $m_0$ consecutive sites starting at position $i_0$. It is well-known that (1) can be mapped to a model of spinless fermions with nearest-neighbour density-density interaction by means of a Jordan-Wigner transformation and all of our results are straightforwardly translated into that setting. The study of local QQs in models of the kind (1) was initiated in 1970 [5], where the noninteracting case $\Delta = 0$, $m_0 = 1$ was shown to lead to a non-thermal stationary state. With the advent of efficient numerical approaches [6, 7], local quenches in the interacting XXZ chain [8, 9] and corresponding conformal field theories [10] have been studied intensely. In the present letter we show that longer quenches $m_0 > 1$ lead to prominent linearly propagating bound states, which in standard condensed matter scenarios have been difficult to discern [9, 11].

We consider the following quench protocol: we prepare the system in the ground state $|0\rangle$ of the Hamiltonian $H(\Delta, B_0 = -\infty)$. At time $t = 0$ we suddenly switch off the magnetic field $B_0$ and then consider the time evolution, governed by the Hamiltonian $H(\Delta, B_0 = 0)$, of the following observables

$$\langle S^z \rangle(j, t) \equiv \langle 0 | S_j^z(t) | 0 \rangle ,$$
$$P_{\uparrow\uparrow}(j, t) \equiv \langle 0 | P_j(t) P_{j+1}(t) | 0 \rangle ,$$
$$P_{\uparrow\uparrow\uparrow}(j, t) \equiv \langle 0 | P_{j-1}(t) P_j(t) P_{j+1}(t) | 0 \rangle , \qquad (2)$$

where $P_j = S_j^z + 1/2$ is the up-spin projection operator on site $j$. In the thermodynamic limit there are different regimes: when the magnetization per site $m$ is equal to $-1/2$ the ground state of $H(\Delta, B_0 = 0)$ is given by the saturated ferromagnetic state with all spins down and a local quench of the type described above then reduces to a quantum mechanical few-body problem. On the other hand, for magnetizations $-1/2 < m < 0$ the model $H(\Delta, B_0 = 0)$ describes a quantum critical (Luttinger liquid) phase and our local quantum quench involves complex many-body effects and can be thought of

as a generalization of the X-ray edge problem. In the following we first consider the simpler, spin-polarized case as this allows us to establish the role played by bound states.

*Spin Polarized Case:* In this case the ground state of $H(\Delta, 0)$ is the ferromagnetic state with all spins down $|\downarrow\rangle$. Excitations with $N_\uparrow$ spin-flips (particles) can be constructed by Bethe's Ansatz and are parametrized by $N_\uparrow$ momenta $k_j$

$$|N_\uparrow, \mathbf{k}\rangle = \sum_{x_1 < \cdots < x_{N_\uparrow}} \Psi(\{k_j\}|\{x_l\}) \prod_{n=1}^{N_\uparrow} S_{x_n}^+ |\downarrow\rangle. \quad (3)$$

Here the wave function $\Psi$ has the characteristic Bethe Ansatz form and the momenta $\{k_j\}$ are subject to quantization conditions, which for a ring geometry read

$$e^{iNk_j} = \prod_{\substack{l=1 \\ l \neq j}}^{N_\uparrow} -\frac{2\Delta e^{ik_j} - 1 - e^{ik_j + ik_l}}{2\Delta e^{ik_l} - 1 - e^{ik_j + ik_l}} \, , \, j = 1, \ldots, N_\uparrow. \quad (4)$$

Energy and momentum are $E = \sum_{j=1}^{N_\uparrow} \epsilon(k_j)$ and $P = \sum_{j=1}^{N_\uparrow} k_j$ respectively, where $\epsilon(k) = J(\cos k - \Delta)$. The solutions $k_j$ of (4) can be either real or complex [12]. The former describe scattering states of "magnons", while the latter correspond to bound states. Bound states involving $\ell$ particles are known as "$\ell$-strings" and have wave functions that exhibit exponential decay (which can be slow) with respect to the distances between particles. Their dispersion relations in the thermodynamic limit are [12, 13] $\epsilon_\ell(k) = -J\frac{\sin(\nu)}{\sin(\ell\nu)}\left(\cos(\ell\nu) - (-1)^\ell \cos(k)\right)$, where $\Delta = \cos(\nu)$. Here the total momentum $k$ of $\ell$-strings is constrained, e.g. for $|\Delta| < 1$ and $\ell = 2$ we have $|k| > 2\nu$. For a given value of $\Delta$ there generally exists a hierarchy of allowed strings, which was first identified in a seminal work by Suzuki and Takahashi [12]. We note that the energy difference between bound states and scattering continua can generally be very small. Using the exact eigenstates of $H(\Delta, 0)$ we can derive a Lehmann representation for the observables (2) after our quench

$$\langle \mathcal{O} \rangle(j, t) = \sum_{\{k_l\}, \{p_r\}} \langle 0|m_0, \mathbf{k}\rangle \langle m_0, \mathbf{k}|\mathcal{O}_1|m_0, \mathbf{p}\rangle \langle m_0, \mathbf{p}|0\rangle$$
$$\times \, e^{-i\sum_{n=1}^{m_0} t[\epsilon(p_n) - \epsilon(k_n)] - (j-1)[p_n - k_n]]} \, , \quad (5)$$

where the sums are over all Bethe Ansatz states with $m_0$ momenta. In the case $m_0 = 1$ an elementary calculation gives $\langle S^z\rangle(j, t) = -\frac{1}{2} + J_{j-1}^2(Jt)$, where $J_n$ is a Bessel function. For large, fixed $j$ this increases exponentially for $Jt \lesssim j$, shows a maximum for $Jt \approx j$ and exhibits an oscillatory power-law decay for $Jt \gtrsim j$. A stationary phase approximation shows that the dominant contribution in the Lehmann representation (5) for $Jt \approx j$ arises from states with $k \approx \frac{\pi}{2}, \frac{3\pi}{2}$, which propagate with the highest possible velocity $v_{\max} = \max_k \left|\frac{\epsilon(k)}{dk}\right| = J$. The
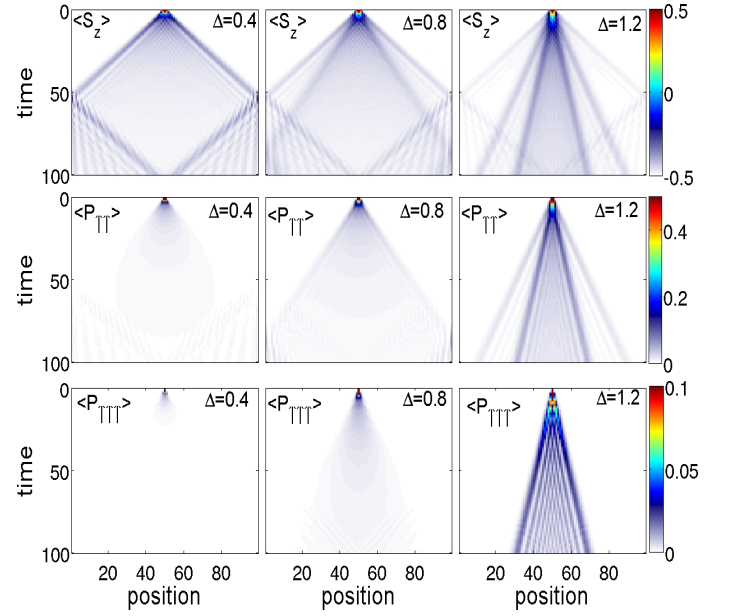


FIG. 1: Time evolution in the spin polarized case after preparing the system in a initial state with three spin flips in the centre of a 101 site chain for different values of $\Delta$. Top row: Spacetime plot of $\langle S^z\rangle(x, t)$; middle row: $\langle \mathcal{P}_{\uparrow\uparrow}\rangle(x, t)$, which projects a bond onto $|\uparrow\uparrow\rangle\langle\uparrow\uparrow|$; bottom row: $\langle \mathcal{P}_{\uparrow\uparrow\uparrow}\rangle(x, t)$, which projects three adjacent sites onto $|\uparrow\uparrow\uparrow\rangle\langle\uparrow\uparrow\uparrow|$.

fact that $\langle S^z\rangle(j, t)$ has a maximum at $Jt \approx j$ can be understood qualitatively by noting that the density of states (DOS) $\rho_1(v) = \int \delta(v - d\epsilon/dk)dk = \frac{N}{2\pi}\frac{1}{\sqrt{J^2 - v^2}}$ has singularities at the maximum speed $v = \pm J$. The exponential supression of $\langle S^z\rangle(j, t)$ for $t \lesssim (j/v_{\max})$ gives rise to a horizon effect and is described by the Lieb-Robinson bound [14].

In all other cases $m_0 > 1$, string states $\ell \geq 2$ will contribute to the time evolution of observables and in order to study their influence we have carried out numerical computations using the TEBD [6]. Results for $m_0 = 3$ (three neighbouring sites with spin up in the initial state) are shown in Fig. 1. As a function of the anisotropy $\Delta$ we observe three distinct regimes, which are fully consistent with expectations from the Bethe ansatz: (i) for small values of $\Delta$ we observe a single wave front in $\langle S^z\rangle(x, t)$, propagating with the maximal magnon velocity $v = J$ (the $m_0 = 1$ case discussed above looks quite similar). (ii) At $\Delta = 0.8$, a second, slower branch of propagating wave packets emerges both in $\langle S^z\rangle(x, t)$ and in $P_{\uparrow\uparrow}(x, t)$ [23]. Its propagation velocity is equal to the maximal 2-string velocity. We have verified by direct evaluation of (5) that the second front is associated with 2-strings. Interestingly there is a threshold in $\Delta$ for observing this phenomenon ($\Delta_c \approx \Delta_0 = 1/\sqrt{2}$), while 2-strings exist at any $\Delta \neq 0$. The reason is that the maximal 2-string velocity is $v_{\max,2} = J\sqrt{1 - \Delta^2}$ for $0 < \Delta < \Delta_0$ and $v_{\max,2} = \frac{J}{2\Delta}$ for $\Delta_0 < \Delta < 1$. On the other hand, the density of
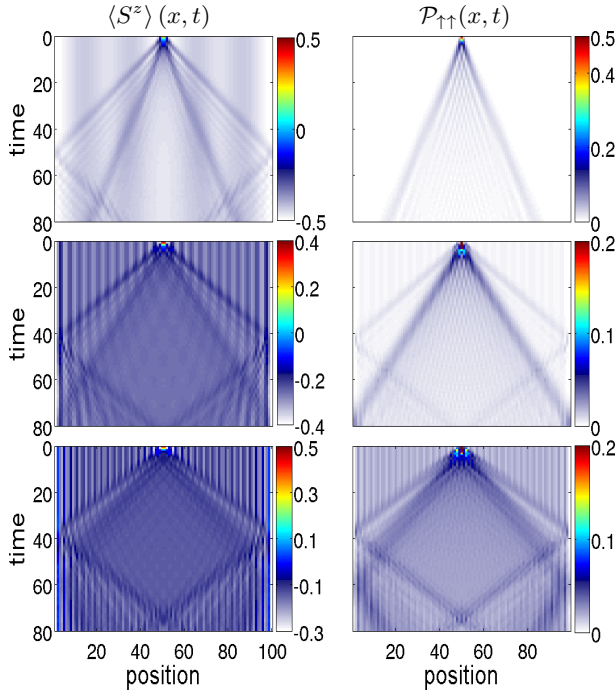
FIG. 2: Two-string propagation at finite magnetization per site $m$ at $\Delta = 1.2$, corresponding to the Luttinger liquid phase of the model. From top to bottom, $m = -0.44$, $m = -0.26$ and $m = -0.14$. The initial state at $t = 0$ is the ground state of (1) with an infinite magnetic field term at two sites in the center of the chain (chain length $N=100$). At $t = 0$, the field is switched off and the state is evolved. The striped patterns visible in all plots are Friedel oscillations due to open boundary conditions.

states for 2-strings is $\rho_2(v) = 2\Delta/\sqrt{J^2 - (2\Delta v)^2}$, which acquires a singularity only if $\Delta > 1/\sqrt{2}$. It is this singularity which induces a clear signature of propagating 2-strings in both $\langle S^z \rangle(x,t)$ and $P_{\uparrow\uparrow}(x,t)$. (iii) For interaction strengths above $\Delta_{c2} \approx 0.9$ we observe an additional branch in $\langle S^z \rangle(x,t)$, $P_{\uparrow\uparrow}(x,t)$ and in $P_{\uparrow\uparrow\uparrow}(x,t)$. This feature clearly arises from propagating 3-strings and can be understood in complete analogy with the 2-string case discussed above.

*Results for Finite Magnetizations:* Here the bulk of our system is in a strongly correlated quantum critical Luttinger liquid phase and our quench protocol described above is closely related to the X-ray edge singularity problem in a correlated host [15]. However, the observables relevant to our case are different and cannot be described using methods of boundary conformal field theory [16]. We computed the quenched ground state using the density matrix renormalization group algorithm [17] and the time evolution using the TEBD with matrix dimensions up to 1200. In Fig. 2 we present results for $\Delta = 1.2$ and three different magnetizations per site $m = (N_\uparrow - N_\downarrow)/2N = -0.44, -0.26, -0.14$, corresponding to $N_\uparrow = 6, 24, 36$ on a $N = 100$ site chain. We note
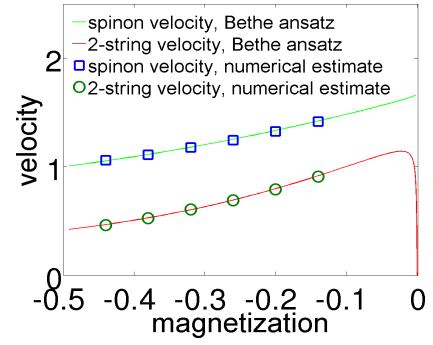


FIG. 3: Propagation velocity of single-spinon and two-string branch as a function of total magnetization per site $m$ of the system at $\Delta = 1.2$. Green and red curves show single-spinon and two-string velocities as calculated from Bethe ansatz. Blue circles and squares are numerically derived values from real time simulations. Errorbars are smaller than symbols.
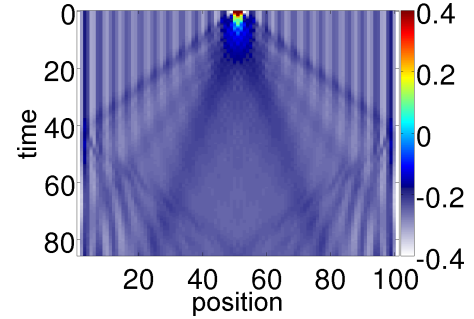


FIG. 4: Spacetime plot of $\langle S^z \rangle$ for a setup similar to Fig. 2 with $N = 101$ at total magnetization $m = -0.2525$, $\Delta = 1.2$, with three particles at the chain center at $t=0$.

that this corresponds to the Luttinger liquid phase of the Heisenberg model even though $\Delta > 1$. In all cases we observe two propagating wave fronts (in each direction) in $\langle S^z \rangle(x,t)$. The results for $P_{\uparrow\uparrow}(x,t)$ show that the slower front is associated with excitations that favour neighbouring spin flips. In order to interpret these results we follow our analysis of the spin polarized case. It is known from the Bethe ansatz solution that the elementary excitations of the Heisenberg chain at finite magnetization are gapless "spinons" as well as gapped bound states associated with string solutions of the Bethe ansatz equations (4). It is then tempting to associate the faster/slower wave fronts with spinon and 2-string excitations respectively, because, just like in the spin polarized case, the latter induce an enhancement in the density of neighbouring spin flips as a result of their bound nature. In order to substantiate this expectation we have evaluated the maximal velocities of both spinon and string excitations as functions of the magnetization per site. In Fig. 3 we present a comparison of these velocities with the ones extracted from the TEBD results in Fig. 2. We see that the results are in excellent agreement.

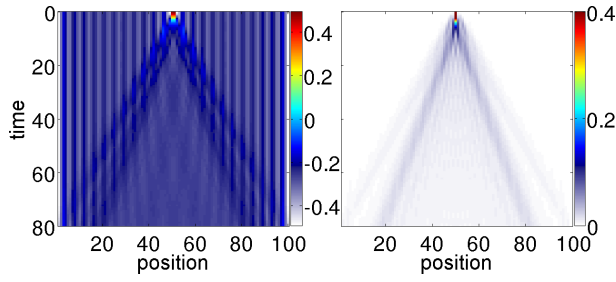For magnetizations closer to zero the two-string branch

FIG. 5: Spacetime plot of $\langle S^z \rangle$ and $P_{\uparrow\uparrow}$ for $N = 100$, $m_0 = 2$ at total magnetization $m = -0.26$, $\Delta = 1.2$ and an extra integrability breaking term $(J/10) \sum_j \mathbf{S}_j \cdot \mathbf{S}_{j+2}$ added to $H(\Delta, B_0)$. Bound state signatures are seen to persist.

gets more and more washed out, because the momentum range of two-string excitations diminishes and eventually vanishes as the magnetization approaches zero [12]. In order to determine whether longer strings also lead to easily recognizable features in observables after a local quench we have analyzed the case $m_0 = 3$ for $\Delta = 1.2$ and magnetization per site $m = -0.2525$. Some results for $\langle S^z \rangle(x,t)$ are shown in Fig. 4. We can now identify three branches. The propagation velocities extracted from the TEBD data are $v_1 \approx 1.26 \pm 0.02$, $v_2 \approx 0.702 \pm 0.025$ and $v_3 \approx 0.370 \pm 0.02$ respectively. These values agree with the maximal velocities of spinons, 2-strings and 3-strings calculated from Bethe ansatz, which are $v_{\max} \approx 1.263$, $v_{\max,2} \approx 0.705$ and $v_{\max,3} \approx 0.375$.

*Integrability breaking perturbations:* In general, string states are not protected kinematically from decaying into scattering states of spinons. Their stability is then a consequence of integrability of the Heisenberg chain and an important question is, whether signatures of bound states survive when integrability breaking perturbations are taken into account. In order to address this issue we have considered two types of perturbation: (i) a next-nearest neighbour interaction and (ii) a spatially varying magnetic field term $\gamma \sum_{j=1}^{N} (j - \frac{N}{2})^2 S_j^z$, which would model an optical trap in certain realizations of (1) based on cold fermionic atoms. In both cases we observe signatures of bound states, indicating that they survive in the form of resonances. We show results for case (i) in Fig. 5.

*Conclusions:* We have studied local quantum quenches in the antiferromagnetic spin-1/2 Heisenberg XXZ chain. We observed that above certain thresholds in the interaction strength $\Delta$, local observables exhibit prominent signatures associated with linearly propagating gapped bound states. Given the difficulty in observing these bound states in scattering experiments on quantum magnets [9, 11] we propose that non-equilibrium setups of the kind considered here are an ideal setting for observing them and probing their properties. Heisenberg spin chains can, e.g., be realized experimentally in crystals and systems of cold atoms in optical lattices with

time and space resolved dynamics [18, 19]. Recent work has focussed on AC driven optical lattices [20] and two-component Bose mixtures [21]. The kind of local perturbation characterizing our initial state could be induced by a focussed laser beam.

---

* Electronic address: evertz@tugraz.at

[1] M. Greiner et al., Nature **419** 51 (2002); S. Hofferberth et. al., Nature **449**, 324 (2007); S. Trotzky et al., arXiv:1101.2659.

[2] T. Kinoshita et. al. Nature **440**, 900 (2006).

[3] J. Dziarmaga, Adv. Phys. **59**, 1063 (2010); A. Polkovnikov et al., Rev. Mod. Phys.**83**, 863 (2011); A. Lamacraft and J.E. Moore, arXiv:1106.3567.

[4] M. Rigol et al., Phys. Rev. Lett. **98**, 50405 (2007); Nature **452**, 854 (2008); P. Calabrese and J. Cardy, Phys. Rev. Lett. **96**, 136801 (2006); J. Stat. Mech. (2007) P06008; (2005) P04010; M. A. Cazalilla, Phys. Rev. Lett. **97**, 156403 (2006); S. R. Manmana et al, Phys. Rev. Lett. **98**, 210405 (2007); M. Cramer et al., Phys. Rev. Lett. **100**, 030602 (2008); T. Barthel and U. Schollwöck, Phys. Rev. Lett. **100**, 100601 (2008); G. Roux, Phys. Rev. A**79**, 021608 (2009); D. Fioretto and G. Mussardo, New J. Phys. **12**, 055015 (2010). C. Kollath et al., Phys. Rev. Lett. **98**, 180601 (2007); G. Biroli et al., Phys. Rev. Lett. **105**, 250401 (2010); D. Rossini et al., Phys. Rev. B**82**, 144302 (2010); P. Calabrese, F.H.L. Essler and M. Fagotti, Phys. Rev. Lett. **106**, 227203 (2011).

[5] D.B. Abraham et. al., Phys. Rev. Lett. **25**, 1449 (1970); Stud. Appl. Math. **50**, 121 (1971).

[6] G. Vidal, Phys. Rev. Lett. **91**, 147902 (2003); *ibid* **93**, 040502 (2004).

[7] A. J. Daley et al., J. Stat. Mech.: Theory Exp (2004) P04005; S. White and A. Feiguin, Phys. Rev. Lett. **93**, 076401 (2004).

[8] D. Gobert et al., Phys. Rev. E **71** , 036102 (2005); D. Petrosyan et al., Phys. Rev. A **76** 033606 (2007); *ibid* **77** 039908(E) (2008); S. Langer et al., Phys. Rev. B **79**, 214409 (2009); J. Ren and S. Zhu, Phys. Rev. A **81**, 014302 (2010); L. F. Santos and A. Mitra, Phys. Rev. E **84**, 016206 (2011); R. Steinigeweg et al., Phys. Rev. Lett. **106** 160602 (2011); S. Langer et al., arXiv:1107.4136.

[9] R. G. Pereira et al., Phys. Rev. Lett. **100**, 027206 (2008).

[10] P. Calabrese and J. Cardy, J. Stat. Mech. P10004 (2007); J.M. Stéphan and J. Dubail, arXiv:1105.4846.

[11] J.-S. Caux and J.-M. Maillet, Phys. Rev. Lett. 95, 077201 (2005); J.-S. Caux et al., J. Stat. Mech. (2005) P09003; R.G. Pereira et al., Phys. Rev. B**79**, 165113 (2009); M. Kohno, Phys. Rev. Lett. **102** 037203 (2009); A. Shashi et. al., Phys. Rev. B.**84**, 045408 (2011); A. Imambekov et al., arXiv:1110.1374.

[12] M. Takahashi and M. Suzuki, Prog. Theor. Phys. **48**,

2187 (1972); M. Fowler and X. Zotos, Phys. Rev. **B24**, 2634 (1981);

[13] B. Sutherland, *Beautiful Models*, World Scientific (2004).

[14] E.H. Lieb and D.W. Robinson, Comm. Math. Phys. 28, 251 (1972).

[15] I. Affleck and A. Ludwig, J. Phys. **A27**, 5375 (1994).

[16] J.L. Cardy, Nucl. Phys. **B324**, 581 (1989).

[17] S.R. White, Phys. Rev. Lett. **69** 2863 (1992); Phys. Rev. B**48**, 10345 (1993).

[18] C. Ramanathan et al., New J. Phys. **13** 103015 (2011).

[19] C. Weitenberg et al., Nature **471** 319 (2011); J. Simon et al., Nature **472**, 7343 (2011); M. Cheneau et al., arXiv:1111.0776.

[20] Y.-A. Chen et al., arXiv:1104.1833.

[21] A.B. Kuklov and B.V. Svistunov, Phys. Rev. Lett. **90**, 100401 (2003); L.-M. Duan et al., Phys. Rev. Lett. **91**,090402 (2003); G. Thalhammer et. al., Phys. Rev. Lett. **100**, 210402 (2008).

[22] The boundary conditions do not affect the propagation noticeably until the wave front reaches the boundary.

[23] We note that these wave fronts, while evident in Fig. 1, are not easy to discern in equal time or space slices due to the oscillatory nature of the signal.